

Article

Reduction of Hg(II) by Fe(II)-Bearing Smectite Clay Minerals

Edward J. O'Loughlin ^{1,*}, Maxim I. Boyanov ^{1,2}, Kenneth M. Kemner ¹
and Korbinian O. Thalhammer ^{1,3}

¹ Biosciences Division, Argonne National Laboratory, Argonne, IL 60439-4843, USA; mboyanov@iche.bas.bg (M.I.B.); kemner@anl.gov (K.M.K.); kthalham@caltech.edu (K.O.T.)

² Institute of Chemical Engineering, Bulgarian Academy of Sciences, 1113 Sofia, Bulgaria

³ Division of Geological and Planetary Sciences, California Institute of Technology, Pasadena, CA 91125, USA

* Correspondence: oloughlin@anl.gov; Tel.: +1-630-252-9902

Received: 28 October 2020; Accepted: 25 November 2020; Published: 1 December 2020



Abstract: Aluminosilicate clay minerals are often a major component of soils and sediments and many of these clays contain structural Fe (e.g., smectites and illites). Structural Fe(III) in smectite clays is redox active and can be reduced to Fe(II) by biotic and abiotic processes. Fe(II)-bearing minerals such as magnetite and green rust can reduce Hg(II) to Hg(0); however, the ability of other environmentally relevant Fe(II) phases, such as structural Fe(II) in smectite clays, to reduce Hg(II) is largely undetermined. We conducted experiments examining the potential for reduction of Hg(II) by smectite clay minerals containing 0–25 wt% Fe. Fe(III) in the clays (SYn-1 synthetic mica-montmorillonite, SWy-2 montmorillonite, NAu-1 and NAu-2 nontronite, and a nontronite from Cheney, Washington (CWN)) was reduced to Fe(II) using the citrate-bicarbonate-dithionite method. Experiments were initiated by adding 500 μM Hg(II) to reduced clay suspensions (4 g clay L^{-1}) buffered at pH 7.2 in 20 mM 3-morpholinopropane-1-sulfonic acid (MOPS). The potential for Hg(II) reduction in the presence of chloride (0–10 mM) and at pH 5–9 was examined in the presence of reduced NAu-1. Analysis of the samples by Hg L_{III} -edge X-ray absorption fine structure (XAFS) spectroscopy indicated little to no reduction of Hg(II) by SYn-1 (0% Fe), while reduction of Hg(II) to Hg(0) was observed in the presence of reduced SWy-2, NAu-1, NAu-2, and CWN (2.8–24.8% Fe). Hg(II) was reduced to Hg(0) by NAu-1 at all pH and chloride concentrations examined. These results suggest that Fe(II)-bearing smectite clays may contribute to Hg(II) reduction in suboxic/anoxic soils and sediments.

Keywords: montmorillonite; nontronite; elemental mercury; reduction

1. Introduction

Mercury (Hg) is present in the environment as a result of natural and anthropogenic processes including mineral weathering, volcanic emission, mining activity, fossil fuel burning, and industrial and consumer use [1,2]. As such, Hg is a common contaminant in many terrestrial and aquatic systems [3,4], and its bioaccumulation in organisms, including humans, is a major environmental concern [5–7]. Although Hg can exist as Hg(II), Hg(I), or Hg(0), Hg(I) is prone to disproportionation and is not commonly found under typical environmental conditions. Hg(II) is particularly soluble in water and can form highly toxic compounds like dimethylmercury as a result of microbial activity [8,9]. Metallic Hg(0) exists as a liquid at room temperature and is also quite toxic, but is considerably less soluble in water than Hg(II). However, due to its low vapor pressure, Hg(0) readily partitions into the atmosphere and is mobile on a global scale. Thus, the reduction of Hg(II) to Hg(0) in soils and sediments, facilitated by both abiotic and microbially-mediated processes, is a key component of the

cycling of Hg between atmospheric and aquatic/terrestrial reservoirs and the overall biogeochemical cycling of Hg [3,9–11].

Iron (Fe) is a highly abundant element in the lithosphere (~5% by mass) and Fe oxides (including formal Fe oxides, oxyhydroxides, and hydroxides such as ferrihydrite ($\text{Fe}_5\text{HO}_8 \cdot 4\text{H}_2\text{O}$), hematite ($\alpha\text{-Fe}_2\text{O}_3$), maghemite ($\gamma\text{-Fe}_2\text{O}_3$), magnetite (Fe_3O_4), goethite ($\alpha\text{-FeOOH}$), lepidocrocite ($\gamma\text{-FeOOH}$)), and Fe-bearing clay minerals (smectites, illites, chlorites, etc.) are common constituents of soils and sediments. The biogeochemistry of Fe in most aquatic and terrestrial environments is driven largely by microbial activity, particularly in Fe-rich soils and sediments where Fe redox cycling by microorganisms is a significant component of C cycling and energy flux [12–16]. Microbial reduction of ferric iron (Fe(III)) can result in the formation of a broad range of Fe(II) species including soluble and adsorbed Fe(II) and mineral phases containing structural Fe(II) (e.g., magnetite, siderite (FeCO_3), vivianite [$\text{Fe}_3(\text{PO}_4)_2 \cdot 8\text{H}_2\text{O}$], green rust, chukanovite [$\text{Fe}_2(\text{OH})_2\text{CO}_3$], and Fe(II)-bearing clays) [17–27]. Fe(II) is one of the most abundant reductants typically present in aquatic and terrestrial environments under suboxic and anoxic conditions [28–30], often providing substantial redox buffering capacity to these systems, and many Fe(II) species are effective reductants for a wide range of organic and inorganic contaminants, including nitroaromatics, chlorinated hydrocarbons, nitrate, heavy metals, and radionuclides [31–42]. In 2003, we reported the reduction of Hg(II) to Hg(0) by green rust [43], a layered redox-reactive Fe(II)-Fe(III) hydroxide with a pyroaurite-type structure. Since then, other Fe(II)-bearing minerals have been shown to reduce Hg(II) to Hg(0), including magnetite [44–47], siderite [48], and mackinawite (FeS) [49], as well as solution phase and adsorbed Fe(II) [50,51]. These results suggest that other Fe(II)-bearing minerals may be effective reductants for Hg(II).

Smectite clays (e.g., montmorillonite, beidellite, nontronite, saponite, and hectorite) are a group of 2:1 (an alumina octahedral sheet bound between two tetrahedral silicate sheets) hydrous aluminum phyllosilicate minerals found in many soils and sediments. Among clay minerals, the high surface area and cation exchange capacity of smectite clays makes them particularly good sorbents for metals including Hg^{2+} [52–57]. Although composed primarily of Si and Al, smectites typically contain Fe (ranging from <1 wt% up to ~30 wt% [58]) due to isomorphic substitution of Fe^{3+} for Si^{4+} in the tetrahedral layer and Fe^{3+} for Al^{3+} in the octahedral layer. As such, smectite clays can be an important component of the Fe pool in soils and sediments. Moreover, the structural Fe(III) in smectites is redox active and can be reduced to Fe(II) by biotic and abiotic processes [59–66]. Although structural Fe(II) in smectite clays has been shown to reduce contaminants including nitroaromatics, chlorinated hydrocarbons, chromate, and pertechnetate [67–74], the ability of clays to reduce Hg(II) is unknown, impeding evaluation of their contribution to the redox cycling of Hg in the environment.

In this study we used X-ray absorption fine structure (XAFS) spectroscopy to examine the potential for reduction of Hg(II) by structural Fe(II) in a suite of smectite clay minerals containing 0–25 wt% structural Fe.

2. Materials and Methods

2.1. Clay Minerals

SYn-1 (Barasym SSM-100, a synthetic mica-montmorillonite), SWy-2 (a Na-rich montmorillonite from Crook County, WY, USA), NAu-1 (a green-colored, Al-enriched nontronite from Uley Mine, South Australia) and NAu-2 (a brown colored, Al-poor nontronite containing tetrahedral Fe from Uley Mine, South Australia) were obtained from the Clay Minerals Society's Source Clays Repository. CWN, a nontronite from Cheney, Washington, USA was purchased from Ward's Natural Sciences Establishment, Inc. SYn-1 and SWy-2 were in powder form and were used as received. Chunks of NAu-1, NAu-2, and CWN were ground in a ball mill. The clays were Na saturated, dispersed, and the clay-sized fraction (<2 μm) isolated by sedimentation as described by O'Loughlin et al. [75] and maintained as an aqueous suspension. The Fe content of the clay-sized fraction was determined by HF

dissolution. A 25 mg dry mass sample of each clay was placed in a 50 mL polypropylene centrifuge tube followed by the addition of 6 mL of 1.8 M H_2SO_4 and 500 μL of 48 wt% HF. The open tubes were placed in a boiling water bath for 30 min. After cooling to ambient temperature, 5 mL of a 5 wt% H_3BO_3 solution was added to neutralize the HF prior to analysis of the Fe concentration by inductively coupled plasma-optical emission spectrometry. Based on this analysis, the clays had the following Fe content (wt%): Barasym (0%), SWy-2 montmorillonite (2.8%), NAu-1 (18.8%), NAu-2 (24.8%), and CWN (21.4%).

2.2. Preparation of Reduced Clays

The clays were reduced (Figure 1) using a modified version of the citrate-bicarbonate-dithionite (CBD) method as described by Ilgen et al. [76]. Briefly, citrate-bicarbonate (CB) buffer solution was prepared by combining 800 mL of 0.3 M sodium citrate with 100 mL of 1 M NaHCO_3 . A volume of clay suspension corresponding to 500 mg dry mass was added to 50 mL of CB buffer and dispersed with mild sonication. The CB/clay suspensions were then transferred to a 240 mL serum bottle, an additional 100 mL of CB buffer was added to each, and the bottles were sparged with Ar to remove O_2 from the suspension and headspace. After sparging for 15 min, 267 mg of sodium dithionite was added, and the bottles were sealed with rubber septa and aluminum crimp caps and placed in a 70 °C water bath for 30 min with periodic mixing. The bottles were then placed in an anoxic glove box (Coy Laboratory Products, Grass Lake, Michigan, 3–5% H_2 in N_2 and Pd catalyst to maintain O_2 in the box <1 ppm) and the CBD-reduced clay suspensions were immediately transferred to 250 mL centrifuge bottles with O-ring closures. The reduced clays were recovered by centrifugation and washed (i.e., resuspension followed by centrifugation) with a series of anoxic solutions over a period of ~6 h as follows: 1 wash with 75 mL of 5 mM NaCl; 2 washes with 75 mL of 2 M NaCl adjusted to pH 4 with 1 M HCl; 1 wash with 75 mL of 5 mM NaCl; and 1 wash with 75 mL of 20 mM 3-morpholinopropane-1-sulfonic acid (MOPS) buffer (pH 7.2). After the final washing, the clays were resuspended in 20 mM pH 7.2 MOPS buffer. All work with the CBD-reduced clays was conducted under anoxic conditions.

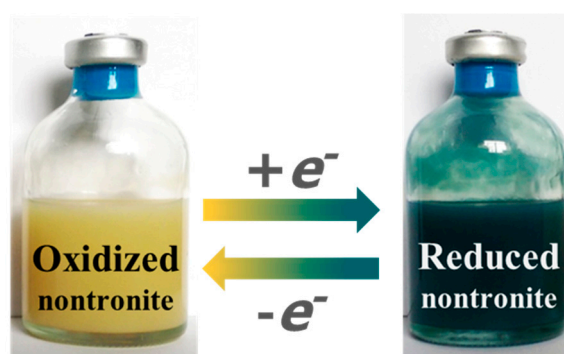


Figure 1. Oxidized and citrate-bicarbonate-dithionite (CBD)-reduced NAu-1 nontronite.

2.3. Experimental Setup

Experiments were initiated by spiking 10 mL of either native or CBD-reduced clay suspensions (4 g clay L^{-1} in pH 7.2 MOPS buffer) in 15-mL polypropylene centrifuge tubes with 500 μL of 10 mM Hg(II) acetate. The tubes were placed on a rotating mixer (Rotamix RKVSD, Appropriate Technical Resources). After 24 h, samples were prepared for XAFS spectroscopy. The suspensions were centrifuged, and the solids were placed inside holes machined in 1.5 mm thick Plexiglass sample holders (slide-mount sample holders) that were then covered with Kapton film held in place with Kapton tape. All work was conducted under anoxic conditions and the samples for XAFS were transferred to the beamline nearby in gas-tight containers.

Using the procedure described above, the effects of pH were examined over the range of pH 5–9 with CBD-reduced NAu-1. Suspensions of NAu-1 were prepared in 20 mM

1,4-diethylpiperazine (DEPP, pH 5.14); 2-morpholinoethanesulfonic acid (MES, pH 6.08); MOPS (pH 7.10); 1,4-piperazinedipropylsulfonic acid (PIPPS, pH 8.09); or DEPP (pH 9.23) and spiked with 500 μL of 10 mM Hg(II). Similarly, the effects of chloride concentration were examined in suspensions of NAu-1 buffered at pH 7.2 in 20 mM MOPS containing either 0, 1, or 10 mM NaCl and spiked with 500 μL of 10 mM Hg(II).

2.4. Hg XAFS Analysis

Hg L_{III}-edge (12,284 eV) XAFS measurements were carried out at the MR-CAT/EnviroCAT insertion device beamline (Sector 10, Advanced Photon Source City State, Abbr (if USA), Country) [77]. X-ray absorption near edge spectra (XANES) and extended X-ray absorption fine structure (EXAFS) spectra were collected in fluorescence mode using gas-filled ionization chambers on samples prepared under anoxic conditions as described above in Section 2.3. Samples were transported in O₂-free containers to the beamline and spectra were collected at $-140\text{ }^{\circ}\text{C}$ within several hours of sample preparation using a Linkam® stage cooled by liquid N₂. The anoxic integrity of samples prepared and analyzed this way has been demonstrated in previous work [78]. Absolute energy calibration was established by setting the inflection point in the spectrum of Au foil to 11,919 eV. Relative energy calibration between samples was maintained by simultaneous in-line scanning a Hg/Sn amalgam sample [45]. Radiation-induced changes in the spectra were not observed at this temperature. Spectra were obtained from up to 10 fresh locations on each sample and averaged to produce the final spectrum.

Analysis of the spectra was based on comparisons to Hg standards. The standards spectra dataset included: hydrated Hg(II) and Hg(II) complexed to acetate in aqueous solution [45]; polycrystalline HgO from Sigma-Aldrich; 2 mM HgClO₄ sorbed to 4 g maghemite L⁻¹ at pH 6.0 [46]; Hg₂Cl₂ (calomel) powder obtained from Sigma-Aldrich; and Hg(0) produced by reduction with ferrous phases (magnetite, green rust) [43,46]. The polycrystalline Hg powders were mounted on the adhesive side of Kapton tape and their absorption spectra were measured in transmission. Solution samples were mounted in a 1.5 mm thick sample holder with Kapton film windows and the spectrum was measured in fluorescence. Adsorbed Hg standards were mounted as wet pastes in a 1.5 mm thick sample holder with Kapton windows and measured in fluorescence mode. Normalization and background removal of the data were done using the program AUTOBK [79].

3. Results and Discussion

3.1. Interaction of Hg(II) with Native and CBD-Reduced Smectites

The reaction of Hg(II) with the native clays is not expected to result in reduction of Hg(II), as a priori the solids have no reducing equivalents to be transferred to Hg (the clay purification process and the reactions with Hg(II) were carried out under ambient (i.e., oxic) conditions). Thus, the spectra measured from the native oxidized solids are expected to represent Hg(II) adsorbed onto the corresponding clays. Figure 2 compares the data to aqueous and solid Hg(II) standards. The edge position and shape of the clay samples is similar to the Hg(II) standards, showing a characteristic “knee” between 12,285 eV and 12,290 eV corresponding to the deep dip and the large second peak in the derivative spectra near 12,287 eV and 12,292 eV, respectively. Although there is speciation-dependent variation in their position and amplitude, these features in the XANES are present in all Hg(II) spectra and have been used for determining Hg(II) in prior work [45,46,48,49]. Therefore, Hg associates with the native clays as adsorbed Hg(II) and these spectra represent the speciation of solid-phase Hg(II) in the absence of redox processes.

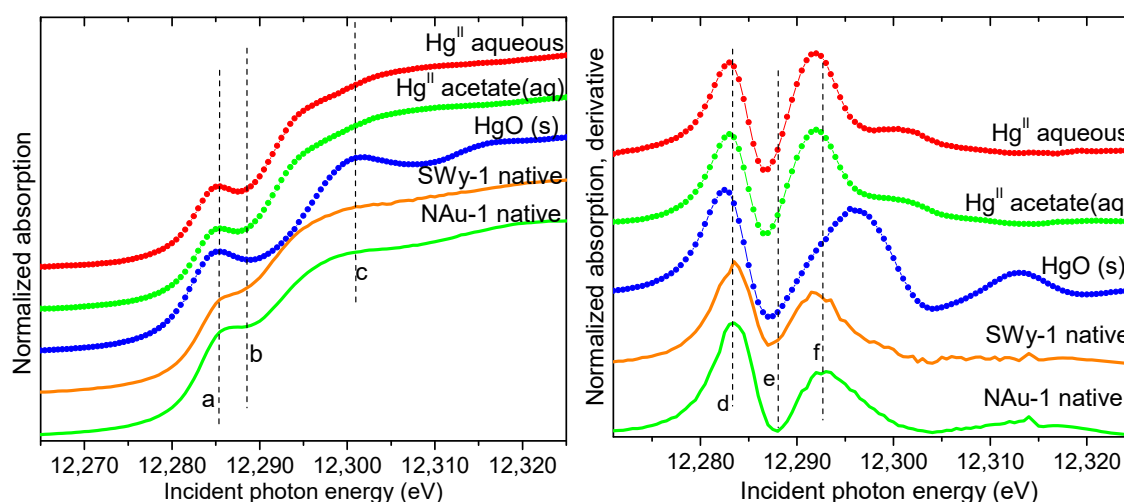


Figure 2. Hg L_{III}-edge XANES spectra (left) and derivative (right) obtained from the solid phase in the systems with native NAu-1 and SWy-2 clays. The spectra are compared to aqueous and solid Hg(II) standards (symbols), which exhibit a deep dip and the large second peak in the derivative spectra (features e and f). The vertical dashed lines (a–f) are a guide to the eye.

The Hg XANES spectra from the CBD-reduced clays reacted with Hg(II) are shown in Figure 3. Relative to the oxidized native clay systems discussed above only the spectrum from Hg(II) reacted with the CBD-reduced Barasym clay (0 wt% Fe) displays the XANES features corresponding to Hg(II); which indicates no reduction of Hg(II) by either Barasym or any potential reductants (e.g., unreacted dithionite) that might not have been removed during the washing procedure following CBD reduction. All other systems with reduced clays (i.e., those containing 2.8–24.8 wt% Fe) lack the “knee” and the features near 12,290 eV indicative of Hg(II). The Hg spectra from the reduced clay systems are identical to that of the Hg(0) standard. Therefore, in all systems with CBD-reduced clays containing Fe (SWy-2, NAu-1, NAu-2, and CWN), Hg(II) was reduced to elemental Hg(0) under the conditions of our study.

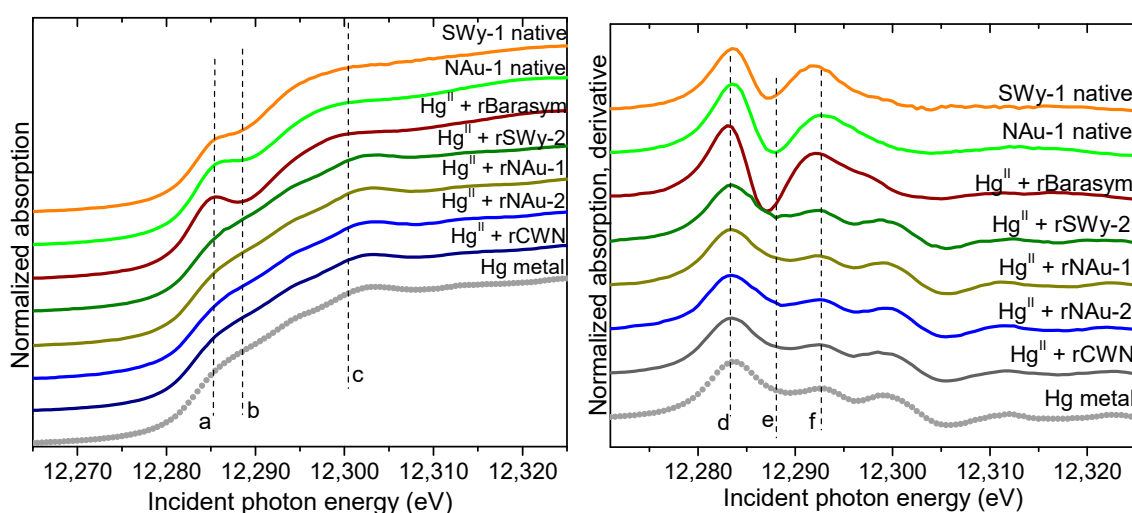


Figure 3. Hg L_{III}-edge XANES spectra (left) and derivative (right) obtained from the solids in systems with clays of different Fe content reduced by the CBD method. Spectra are compared to that of Hg(II) in the native (un-reduced) clays and to the Hg(0) standard (symbols). The vertical dashed lines (a–f) are a guide to the eye, delineating features corresponding to the different valence states of Hg.

3.2. Effect of pH on Hg(II) Reduction by CBD-Reduced NAu-1

The pH of natural systems can vary broadly, so we examined the potential for reduction of Hg(II) by CBD-reduced NAu-1 at pH values from 5–9, a range representative of the majority of aquatic and terrestrial environments. The XANES spectra from the CBD-reduced NAu-1 clay reacted with Hg(II) at pH 5, 6, 7, 8, and 9 are shown in Figure 4. Relative to the native NAu-1 clay system where Hg was associated with the solids as adsorbed Hg(II), the spectra of Hg in the reduced NAu-1 solids were identical to that of the Hg(0) standard. Therefore, the reduction of Hg(II) by Fe(II) in reduced NAu-1 clays was possible at all pH values between 5 and 9 under the conditions of our experiments and the resulting species was elemental Hg(0).

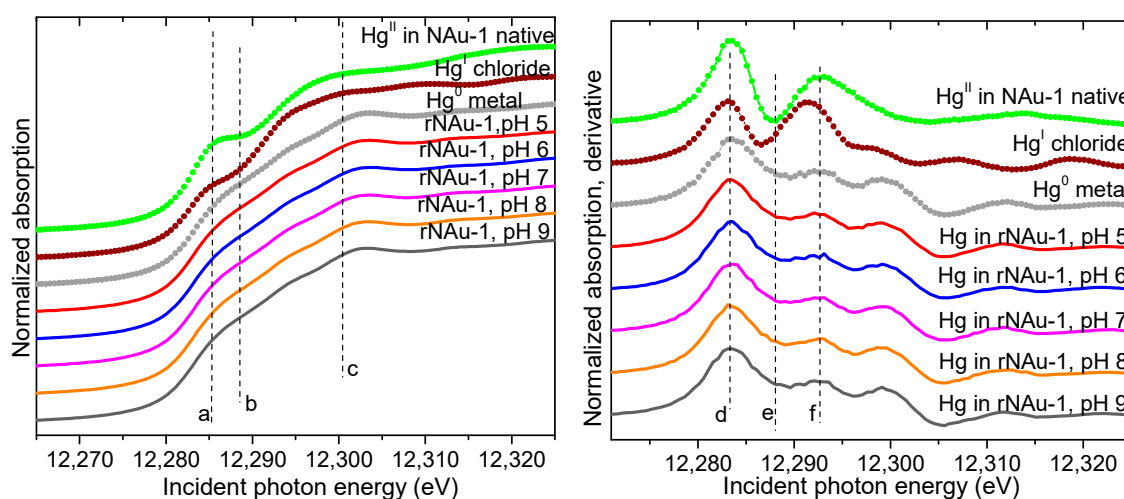


Figure 4. Hg L_{III}-edge XANES spectra (**left**) and derivative (**right**) from the solids in the rNAu-1 systems at pH 5–9 compared to standards (symbols). The vertical dashed lines (a–f) are a guide to the eye, delineating features corresponding to the different valence states of Hg.

3.3. Effect of Chloride Concentration on Hg(II) Reduction by CBD-Reduced NAu-1

Chloride (Cl⁻) is ubiquitous in aquatic and terrestrial environments and is known to form strong aqueous complexes with Hg(II) [80]. The formation of these complexes (e.g., HgCl⁺, HgCl₂, HgCl₃⁻, and HgCl₄²⁻) can influence the behavior of Hg(II), including inhibition of Hg(II) reduction [44,46,81–83] and sorption on clays, metal oxides, and natural sediments [53,84–87]. Previous work has shown that the presence of Cl⁻ in a reducing Fe(II)/(III)-oxide system can prevent complete reduction of Hg(II) to Hg(0) and promote formation of metastable Hg(I) as calomel (Hg₂Cl₂) [46]. We tested for potential effects of Cl⁻ on Hg(II) reduction by CBD-reduced NAu-1 clay at Cl⁻ concentrations of 0, 1, and 10 mM; which covers the range of Cl⁻ concentrations typical of freshwaters, near-surface groundwater, and soils. The XANES derivative spectra from these systems are compared to standards in Figure 5. The spectra lack the deep minimum near 12,287 eV and the second maximum near 12,292 eV that are characteristic of the Hg(II) and Hg(I) standards. Instead, the spectra at all Cl⁻ concentrations are identical to the Hg(0) standard. Therefore, the presence of Cl⁻ did not result in calomel formation and Hg(II) was reduced to elemental Hg(0) under the conditions of these experiments. However, given that Hg(I) species are generally metastable, it is important to note that the lack of detection of Hg(I) in the 1 and 10 mM Cl⁻ systems does not preclude its formation and subsequent disappearance prior to the XAFS measurements of the solids made 24 h after exposure of Hg(II) to the CBD-reduced clay.

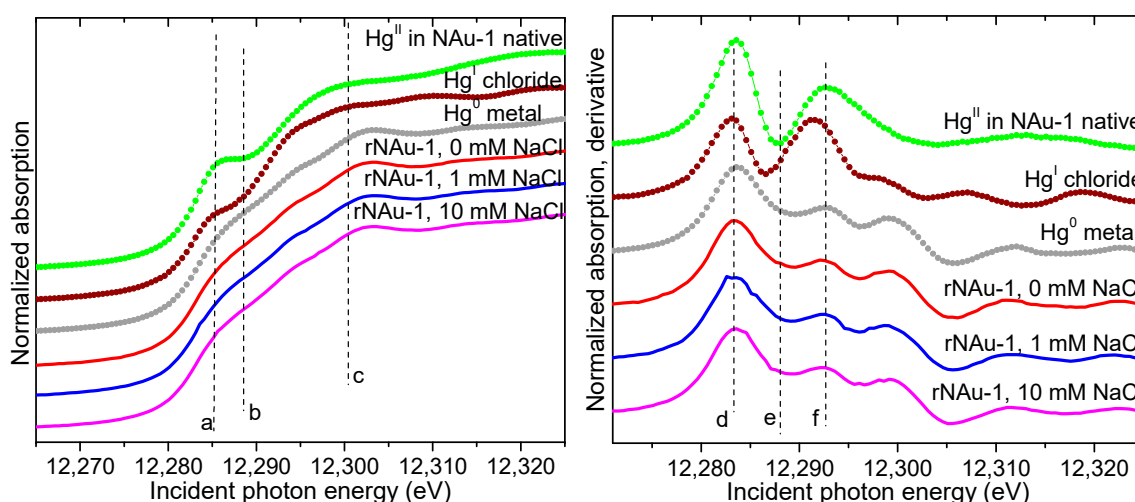


Figure 5. Hg L_{III}-edge XANES spectra (**left**) and derivative (**right**) from the solids in the rNAu-1 systems with increasing NaCl concentrations compared to standards (symbols). The vertical dashed lines (a–f) are a guide to the eye, delineating features corresponding to the different valences of Hg.

3.4. Environmental Relevance

Emission of Hg(0) from aquatic and terrestrial systems to the atmosphere is a major component of the global biogeochemical Hg cycle and reduction of Hg(II) to Hg(0) in soils and sediments is a fundamental part of this process [8–10]. However, the mechanisms of the reduction of Hg(II) to Hg(0) in soils and sediments are not fully understood [9]. Photochemical reduction of Hg(II) can occur in surface waters and at the soil surface [88–90] and the dark reduction of Hg(II) can occur via biotic and abiotic processes. Many microbes common to aquatic and terrestrial environments can enzymatically reduce Hg(II) to Hg(0), primarily as an inducible detoxification mechanism [91,92], although in some dissimilatory Fe(III)-reducing bacteria the ability to reduce Hg(II) is constitutive and involves the respiratory electron transport chain [93,94]. In addition, natural organic matter (NOM), including humic and fulvic acids, can reduce Hg(II) to Hg(0) [82,95–99]. Furthermore, the activity of Fe(III)-reducing microbes in soils and sediments generates Fe(II) species that can reduce Hg(II) to Hg(0) [43–46,48–51]—including structural Fe(II) in smectite clays as shown in this study—creating the possibility for coupled biotic–abiotic Hg(II) reduction pathways under Fe(III)-reducing conditions. Indeed, Peretyazhko et al. reported reduction of Hg(II) to Hg(0) by biogenic Fe(II) in a hydromorphic tropical soil [100]. Similarly, Debure et al. attributed reduction of Hg(II) to Hg(0) in anoxic subsurface sediments to the presence of magnetite and siderite [101], and Poulin et al., reported a correlation between aqueous Hg(0) concentrations and products of microbial Fe/Mn reduction in a riparian soil impacted by historic Hg contamination [102]. Given that Fe-bearing clays are common constituents of many soils and sediment and that structural Fe(II) in clays has been shown to reduce a broad range of organic and inorganic contaminants, it is reasonable to expect that they might contribute to Hg(II) reduction and subsequent Hg(0) emission in situ.

Our results showing the reduction of Hg(II) to Hg(0) by structural Fe(II) in smectite clay minerals increases the number of known Fe(II) species that can reduce Hg(II). However, fundamental aspects of this reaction need to be explored including: the reaction kinetics; the effects of Hg(II) complexation by NOM, minerals, and microbes; the presence of competing electron acceptors (e.g., molecular oxygen and nitrate); and the potential reactivity of structural Fe(II) in other phyllosilicate clay minerals (e.g., illites, vermiculites, etc.). Moreover, the reduction of Fe(II) in smectite clays in near-surface environments is likely to be due primarily to microbial activity, particularly by Fe(III)-reducing bacteria and archaea, and in laboratory studies the dynamics of Fe(II) speciation and clay mineralogy are often quite different during microbial reduction (or simulation of microbial reduction by the addition of Fe(II)) compared to strictly abiotic reduction (e.g., by dithionite as in this study) of structural

Fe(III) [62,63,65,103–107]. As such, additional studies focused on the dynamics of Hg(II) during microbial reduction of Fe(III)-bearing smectite clays are needed.

Author Contributions: Conceptualization E.J.O.; formal analysis M.I.B.; funding acquisition M.I.B., K.M.K., and E.J.O.; Investigation M.I.B., K.M.K., E.J.O., and K.O.T.; Project administration E.J.O.; Visualization M.I.B.; writing—original draft M.I.B. and E.J.O.; and writing—review and editing M.I.B., K.M.K., E.J.O., and K.O.T. All authors have read and agreed to the published version of the manuscript.

Funding: Research under the Wetlands Hydrobiogeochemistry Scientific Focus Area (SFA) at Argonne National Laboratory was supported by the Subsurface Biogeochemical Research Program, Office of Biological and Environmental Research (BER), Office of Science, U.S. Department of Energy (DOE), under contract DE-AC02-06CH11357. MRCAT/EnviroCAT operations are supported by DOE and the member institutions. Use of the Advanced Photon Source, an Office of Science User Facility operated for the U.S. Department of Energy (DOE) Office of Science by Argonne National Laboratory, was supported by the U.S. DOE under Contract No. DE-AC02-06CH11357. Argonne National Laboratory is a U.S. Department of Energy laboratory managed by UChicago Argonne, LLC.

Acknowledgments: We thank the MRCAT beamline staff for assistance during data collection at the synchrotron and the four anonymous reviewers for their thoughtful comments.

Conflicts of Interest: The authors declare no conflict of interest. The funders had no role in the design of the study; in the collection, analyses, or interpretation of data; in the writing of the manuscript, or in the decision to publish the results.

References

1. Fitzgerald, W.F.; Lamborg, C.H. Geochemistry of mercury in the environment. In *Environmental Geochemistry*; Lollar, B.S., Ed.; Elsevier: Amsterdam, The Netherlands, 2003; Volume 9, pp. 107–148.
2. Beckers, F.; Rinklebe, J. Cycling of mercury in the environment: Sources, fate, and human health implications: A review. *Crit. Rev. Environ. Sci. Technol.* **2017**, *47*, 693–794. [[CrossRef](#)]
3. Stein, E.D.; Cohen, Y.; Winer, A.M. Environmental distribution and transformation of mercury compounds. *Crit. Rev. Environ. Sci. Technol.* **1996**, *26*, 1–43. [[CrossRef](#)]
4. Wang, Q.; Kim, D.; Dionysiou, D.D.; Sorial, G.A.; Timberlake, D. Sources and remediation for mercury contamination in aquatic systems—A literature review. *Environ. Pollut.* **2004**, *131*, 323–336. [[CrossRef](#)] [[PubMed](#)]
5. Boening, D.W. Ecological effects, transport, and fate of mercury: A general review. *Chemosphere* **2000**, *40*, 1335–1351. [[CrossRef](#)]
6. Mergler, D.; Anderson, H.A.; Chan, L.H.M.; Mahaffey, K.R.; Murray, M.; Sakamoto, M.; Stern, A.H. Methylmercury exposure and health effects in humans: A worldwide concern. *Ambio J. Hum. Environ.* **2007**, *36*, 3–11. [[CrossRef](#)]
7. Kim, K.H.; Kabir, E.; Jahan, S.A. A review on the distribution of Hg in the environment and its human health impacts. *J. Hazard. Mater.* **2016**, *306*, 376–385. [[CrossRef](#)] [[PubMed](#)]
8. Morel, F.M.M.; Kraepiel, A.M.L.; Amyot, M. The chemical cycle and bioaccumulation of mercury. *Annu. Rev. Ecol. Syst.* **1998**, *29*, 543–566. [[CrossRef](#)]
9. O'Driscoll, N.J.; Rencz, A.; Lean, D.R.S. The biogeochemistry and fate of mercury in the environment. In *Metal Ions in Biological Systems*; Sigel, A., Sigel, H., Sigel, R.K.O., Eds.; Taylor and Francis Group: Boca Raton, FL, USA, 2005; Volume 43, pp. 221–238.
10. Schlüter, K. Review: Evaporation of mercury from soils. An integration and synthesis of current knowledge. *Environ. Geol.* **2000**, *39*, 249–271. [[CrossRef](#)]
11. Selin, N.E. Global biogeochemical cycling of mercury: A review. *Annu. Rev. Environ. Resour.* **2009**, *34*, 43–63. [[CrossRef](#)]
12. Canfield, D.E.; Thamdrup, B.; Hansen, J.W. The anaerobic degradation of organic matter in Danish coastal sediments: Iron reduction, manganese reduction, and sulfate reduction. *Geochim. Cosmochim. Acta* **1993**, *57*, 3867–3883. [[CrossRef](#)]
13. Nealson, K.H.; Saffarini, D.A. Iron and manganese in anaerobic respiration: Environmental significance, physiology, and regulation. *Annu. Rev. Microbiol.* **1994**, *48*, 311–343. [[CrossRef](#)] [[PubMed](#)]

14. Roden, E.E.; Wetzell, R.G. Organic carbon oxidation and methane production by microbial Fe(III) oxide reduction in vegetated and unvegetated freshwater wetland sediments. *Limnol. Oceanogr.* **1996**, *41*, 1733–1748. [[CrossRef](#)]
15. Lovley, D.R. Fe(III) and Mn(IV) reduction. In *Environmental Microbe-Metal Interactions*; Lovley, D.R., Ed.; American Society for Microbiology Press: Washington, DC, USA, 2000; pp. 3–30.
16. Thamdrup, B. Bacterial manganese and iron reduction in aquatic sediments. *Adv. Microb. Ecol.* **2000**, *16*, 41–84.
17. Lovley, D.R.; Stolz, J.F.; Nord, G.L., Jr.; Phillips, E.J.P. Anaerobic production of magnetite by a dissimilatory iron-reducing microorganism. *Nature* **1987**, *330*, 252–254. [[CrossRef](#)]
18. Fredrickson, J.K.; Zachara, J.M.; Kennedy, D.W.; Dong, H.; Onstott, T.C.; Hinman, N.W.; Li, S.-M. Biogenic iron mineralization accompanying the dissimilatory reduction of hydrous ferric oxide by a groundwater bacterium. *Geochim. Cosmochim. Acta* **1998**, *62*, 3239–3257. [[CrossRef](#)]
19. Ona-Nguema, G.; Abdelmoula, M.; Jorand, F.; Benali, O.; Géhin, A.; Block, J.-C.; Génin, J.-M.R. Iron(II,III) hydroxycarbonate green rust formation and stabilization from lepidocrocite bioreduction. *Environ. Sci. Technol.* **2002**, *36*, 16–20. [[CrossRef](#)]
20. Glasauer, S.; Weidler, P.G.; Langley, S.; Beveridge, T.J. Controls on Fe reduction and mineral formation by a subsurface bacterium. *Geochim. Cosmochim. Acta* **2003**, *67*, 1277–1288. [[CrossRef](#)]
21. Roh, Y.; Zhang, C.-L.; Vali, H.; Lauf, R.J.; Zhou, J.; Phelps, T.J. Biogeochemical and environmental factors in Fe biomineralization: Magnetite and siderite formation. *Clays Clay Miner.* **2003**, *51*, 83–95. [[CrossRef](#)]
22. Kukkadapu, R.K.; Zachara, J.M.; Fredrickson, J.K.; Kennedy, D.W.; Dohnalkova, A.C.; Mccready, D.E. Ferrous hydroxy carbonate is a stable transformation product of biogenic magnetite. *Am. Mineral.* **2005**, *90*, 510–515. [[CrossRef](#)]
23. Behrends, T.; Van Cappellen, P. Transformation of hematite into magnetite during dissimilatory iron reduction—conditions and mechanisms. *Geomicrobiol. J.* **2007**, *24*, 403–416. [[CrossRef](#)]
24. Boyanov, M.I.; O’Loughlin, E.J.; Kemner, K.M. Iron phase transformations resulting from the respiration of *Shewanella putrefaciens* on a mixed mineral phase. *J. Phys. Conf. Ser.* **2009**, *190*, 1–4. [[CrossRef](#)]
25. Shelobolina, E.; Konishi, H.; Xu, H.; Benzine, J.; Xiong, M.Y.; Wu, T.; Blothe, M.; Roden, E. Isolation of phyllosilicate-iron redox cycling microorganisms from an illite-smectite rich hydromorphic soil. *Front. Microbiol.* **2012**, *3*, 134. [[CrossRef](#)] [[PubMed](#)]
26. O’Loughlin, E.J.; Gorski, C.A.; Scherer, M.M. Effects of phosphate on secondary mineral formation during the bioreduction of akaganeite (β -FeOOH): Green rust versus framboidal magnetite. *Curr. Inorg. Chem.* **2015**, *5*, 214–224. [[CrossRef](#)]
27. O’Loughlin, E.J.; Gorski, C.A.; Flynn, T.M.; Scherer, M.M. Electron donor utilization and secondary mineral formation during the bioreduction of lepidocrocite by *Shewanella putrefaciens* CN32. *Minerals* **2019**, *9*, 434. [[CrossRef](#)]
28. Hering, J.G.; Stumm, W. Oxidative and reductive dissolution of minerals. In *Mineral-Water Interface Geochemistry*; Hochella, M.F.J., White, A.F., Eds.; American Mineralogical Society: Washington, DC, USA, 1990; Volume 23, pp. 427–465.
29. Lyngkilde, J.; Christensen, T.H. Redox zones of a landfill leachate pollution plume (Vejen, Denmark). *J. Contam. Hydrol.* **1992**, *10*, 273–289. [[CrossRef](#)]
30. Rügge, K.; Hofstetter, T.B.; Haderlein, S.B.; Bjerg, P.L.; Knudsen, S.; Zraunig, C.; Mosbæk, H.; Christensen, T.H. Characterization of predominant reductants in an anaerobic leachate-contaminated aquifer by nitroaromatic probe compounds. *Environ. Sci. Technol.* **1998**, *32*, 23–31. [[CrossRef](#)]
31. Cui, D.; Eriksen, T.E. Reduction of pertechnetate in solution by heterogeneous electron transfer from Fe(II)-containing geological material. *Environ. Sci. Technol.* **1996**, *30*, 2263–2269. [[CrossRef](#)]
32. Patterson, R.R.; Fendorf, S.E.; Fendorf, M.J. Reduction of hexavalent chromium by amorphous iron sulfide. *Environ. Sci. Technol.* **1997**, *31*, 2039–2044. [[CrossRef](#)]
33. Hansen, H.C.B.; Koch, C.B.; Nancke-Krogh, H.; Borggaard, O.K.; Sorensen, J. Abiotic nitrate reduction to ammonium: Key role of green rust. *Environ. Sci. Technol.* **1996**, *30*, 2053–2056. [[CrossRef](#)]
34. Elsner, M.; Schwarzenbach, R.P.; Haderlein, S.B. Reactivity of Fe(II)-bearing minerals toward reductive transformation of organic contaminants. *Environ. Sci. Technol.* **2004**, *38*, 799–807. [[CrossRef](#)]
35. Lee, W.; Batchelor, B. Reductive capacity of natural reductants. *Environ. Sci. Technol.* **2003**, *37*, 535–541. [[CrossRef](#)] [[PubMed](#)]

36. Nakata, K.; Nagasaki, S.; Tanaka, S.; Sakamoto, Y.; Tanaka, T.; Ogawa, H. Reduction rate of neptunium(V) in heterogeneous solution with magnetite. *Radiochim. Acta* **2004**, *92*, 145–149. [[CrossRef](#)]
37. Powell, B.A.; Fjeld, R.A.; Kaplan, D.I.; Coates, J.T.; Serkiz, S.M. Pu(V)O₂⁺ adsorption and reduction by synthetic magnetite. *Environ. Sci. Technol.* **2004**, *38*, 6016–6024. [[CrossRef](#)] [[PubMed](#)]
38. Williams, A.G.B.; Gregory, K.B.; Parkin, G.F.; Scherer, M.M. Hexahydro-1,3,5-trinitro-1,3,5-triazine transformation by biologically reduced ferrihydrite: Evolution of Fe mineralogy, surface area, and reaction rates. *Environ. Sci. Technol.* **2005**, *39*, 5183–5189. [[CrossRef](#)] [[PubMed](#)]
39. Scheinost, A.C.; Charlet, L. Selenite reduction by mackinawite, magnetite and siderite: XAS characterization of nanosized redox products. *Environ. Sci. Technol.* **2008**, *42*, 1984–1989. [[CrossRef](#)]
40. O’Loughlin, E.J.; Kelly, S.D.; Kemner, K.M. XAFS investigation of the interactions of U^{VI} with secondary mineralization products from the bioreduction of Fe^{III} oxides. *Environ. Sci. Technol.* **2010**, *44*, 1656–1661. [[CrossRef](#)]
41. Kwon, M.J.; O’Loughlin, E.J.; Antonopoulos, D.; Finneran, K.T. Geochemical and microbiological processes contributing to the transformation of hexahydro-1,3,5-trinitro-1,3,5-triazine (RDX) in contaminated aquifer material. *Chemosphere* **2011**, *84*, 1223–1230. [[CrossRef](#)]
42. Yan, S.; Boyanov, M.I.; Mishra, B.; Kemner, K.M.; O’Loughlin, E.J. U(VI) reduction by biogenic and abiotic hydroxycarbonate green rusts: Impacts on U(IV) speciation and stability over time. *Environ. Sci. Technol.* **2018**, *52*, 4601–4609. [[CrossRef](#)]
43. O’Loughlin, E.J.; Kelly, S.D.; Kemner, K.M.; Csencsits, R.; Cook, R.E. Reduction of Ag^I, Au^{III}, Cu^{II}, and Hg^{II} by Fe^{II}/Fe^{III} hydroxysulfate green rust. *Chemosphere* **2003**, *53*, 437–446. [[CrossRef](#)]
44. Wiatrowski, H.A.; Das, S.; Kukkadapu, R.; Ilton, E.S.; Barkay, T.; Yee, N. Reduction of Hg(II) to Hg(0) by magnetite. *Environ. Sci. Technol.* **2009**, *43*, 5307–5313. [[CrossRef](#)]
45. Mishra, B.; O’Loughlin, E.J.; Boyanov, M.I.; Kemner, K.M. Binding of Hg^{II} to high-affinity sites on bacteria inhibits reduction to Hg⁰ by mixed Fe^{II/III} phases. *Environ. Sci. Technol.* **2011**, *45*, 9597–9603. [[CrossRef](#)] [[PubMed](#)]
46. Pasakarnis, T.S.; Boyanov, M.I.; Kemner, K.M.; Mishra, B.; O’Loughlin, E.J.; Parkin, G.; Scherer, M.M. Influence of chloride and Fe(II) content on the reduction of Hg(II) by magnetite. *Environ. Sci. Technol.* **2013**, *47*, 6987–6994. [[CrossRef](#)] [[PubMed](#)]
47. Liu, S.; Wiatrowski, H.A. Reduction of Hg(II) to Hg(0) by biogenic magnetite from two magnetotactic bacteria. *Geomicrobiol. J.* **2017**, *35*, 198–208. [[CrossRef](#)]
48. Ha, J.; Zhao, X.; Yu, R.; Barkay, T.; Yee, N. Hg(II) reduction by siderite (FeCO₃). *Appl. Geochem.* **2017**, *78*, 211–218. [[CrossRef](#)]
49. Bone, S.E.; Bargar, J.R.; Sposito, G. Mackinawite (FeS) reduces mercury(II) under sulfidic conditions. *Environ. Sci. Technol.* **2014**, *48*, 10681–10689. [[CrossRef](#)]
50. Charlet, L.; Bosbach, D.; Peretyashko, T. Natural attenuation of TCE, As, Hg, linked to the heterogeneous oxidation of Fe(II): An AFM study. *Chem. Geol.* **2002**, *190*, 303–319. [[CrossRef](#)]
51. Amirbahman, A.; Kent, D.B.; Curtis, G.P.; Marvin-Dipasquale, M.C. Kinetics of homogeneous and surface-catalyzed mercury(II) reduction by iron(II). *Environ. Sci. Technol.* **2013**, *47*, 7204–7213. [[CrossRef](#)]
52. Brigatti, M.F.; Colonna, S.; Malferrari, D.; Medici, L.; Poppi, L. Mercury adsorption by montmorillonite and vermiculite: A combined XRD, TG-MS, and EXAFS study. *Appl. Clay Sci.* **2005**, *28*, 1–8. [[CrossRef](#)]
53. Green-Ruiz, C. Effect of salinity and temperature on the adsorption of Hg(II) from aqueous solutions by a Ca-montmorillonite. *Environ. Technol.* **2009**, *30*, 63–68. [[CrossRef](#)]
54. Guerra, D.L.; Santos, M.R.M.C.; Airoldi, C. Mercury adsorption on natural and organofunctionalized smectites-thermodynamics of cation removal. *J. Braz. Chem. Soc.* **2009**, *20*, 594–603. [[CrossRef](#)]
55. Praus, P.; Montáková, M.; Ritz, M. Montmorillonite ion exchanged by mercury(II). *Acta Geodyn. Geomater.* **2012**, *9*, 63–70.
56. Guerra, D.L.; Silva, R.A.R.; Mello, I. Adsorption of mercury from aqueous solution by nontronite, *Aspergillus niger*, and hybrid material. *Water Qual. Res. J.* **2013**, *48*, 155–170. [[CrossRef](#)]
57. do Nascimento, F.H.; Masini, J.C. Influence of humic acid on adsorption of Hg(II) by vermiculite. *J. Environ. Manag.* **2014**, *143*, 1–7. [[CrossRef](#)] [[PubMed](#)]
58. Amonette, J.E. Iron redox chemistry of clays and oxides: Environmental applications. In *Electrochemical Properties of Clays*; Fitch, A., Ed.; The Clay Minerals Society: Aurora, CO, USA, 2002; Volume 10, pp. 89–147.

59. Rozenon, I.; Heller-Kallai, L. Reduction and oxidation of Fe^{3+} in dioctahedral smectites-1: Reduction with hydrazine and dithionite. *Clays Clay Miner.* **1976**, *24*, 271–282. [[CrossRef](#)]
60. Rozenon, I.; Heller-Kallai, L. Reduction and oxidation of Fe^{3+} in dioctahedral smectites-2: Reduction with sodium sulphide solutions. *Clays Clay Miner.* **1976**, *24*, 283–288. [[CrossRef](#)]
61. Stucki, J.W.; Golden, D.C.; Roth, C.B. Preparation and handling of dithionite-reduced smectite suspensions. *Clays Clay Miner.* **1984**, *32*, 191–197. [[CrossRef](#)]
62. Kostka, J.E.; Haefele, E.; Viehweger, R.; Stucki, J.W. Respiration and dissolution of iron(III)-containing clay minerals by bacteria. *Environ. Sci. Technol.* **1999**, *33*, 3127–3133. [[CrossRef](#)]
63. Jaisi, D.P.; Dong, H.; Liu, C. Influence of biogenic Fe(II) on the extent of microbial reduction of Fe(III) in clay minerals nontronite, illite, and chlorite. *Geochim. Cosmochim. Acta* **2007**, *71*, 1145–1158. [[CrossRef](#)]
64. Kashefi, K.; Shelobolina, E.S.; Elliott, W.C.; Lovley, D.R. Growth of thermophilic and hyperthermophilic Fe(III)-reducing microorganisms on a ferruginous smectite as the sole electron acceptor. *Appl. Environ. Microbiol.* **2008**, *74*, 251–258. [[CrossRef](#)]
65. Dong, H.; Jaisi, D.P.; Kim, J.; Zhang, G. Microbe-clay mineral interactions. *Am. Mineral.* **2009**, *94*, 1505–1519. [[CrossRef](#)]
66. Gorski, C.A.; Aeschbacher, M.; Soltermann, D.; Voegelin, A.; Baeyens, B.; Fernandes, M.M.; Hofstetter, T.B.; Sander, M. Redox properties of structural Fe in clay minerals. 1. Electrochemical quantification of electron-donating and -accepting capacities of smectites. *Environ. Sci. Technol.* **2012**, *46*, 9360–9368. [[CrossRef](#)] [[PubMed](#)]
67. Taylor, R.W.; Shen, S.; Bleam, W.F.; Tu, S.-I. Chromate removal by dithionate-reduced clays: Evidence from direct x-ray adsorption near edge spectroscopy (XANES) of chromate reduction at clay surfaces. *Clays Clay Miner.* **2000**, *48*, 648–654. [[CrossRef](#)]
68. Cervini-Silva, J.; Larson, R.A.; Wu, J.; Stucki, J.W. Transformation of chlorinated aliphatic compounds by ferruginous smectite. *Environ. Sci. Technol.* **2001**, *35*, 805–809. [[CrossRef](#)] [[PubMed](#)]
69. Hofstetter, T.B.; Schwarzenbach, R.P.; Haderlein, S.B. Reactivity of Fe(II) species associated with clay minerals. *Environ. Sci. Technol.* **2003**, *37*, 519–528. [[CrossRef](#)] [[PubMed](#)]
70. Neumann, A.; Hofstetter, T.B.; Skarpeli-Liati, M.; Schwarzenbach, R.P. Reduction of polychlorinated ethanes and carbon tetrachloride by structural Fe(II) in smectites. *Environ. Sci. Technol.* **2009**, *43*, 4082–4089. [[CrossRef](#)]
71. Bishop, M.E.; Dong, H.; Kukkadapu, R.K.; Liu, C.; Edelman, R.E. Bioreduction of Fe-bearing clay minerals and their reactivity toward pertechnetate (Tc-99). *Geochim. Cosmochim. Acta* **2011**, *75*, 5229–5246. [[CrossRef](#)]
72. Bishop, M.E.; Glasser, P.; Dong, H.; Arey, B.; Kovarik, L. Reduction and immobilization of hexavalent chromium by microbially reduced Fe-bearing clay minerals. *Geochim. Cosmochim. Acta* **2014**, *133*, 186–203. [[CrossRef](#)]
73. Luan, F.; Liu, Y.; Griffin, A.M.; Gorski, C.A.; Burgos, W.D. Iron(III)-bearing clay minerals enhance bioreduction of nitrobenzene by *Shewanella putrefaciens* CN32. *Environ. Sci. Technol.* **2015**, *49*, 1418–1426. [[CrossRef](#)]
74. Joe-Wong, C.; Brown, G.E., Jr.; Maher, K. Kinetics and products of chromium(VI) reduction by iron(II/III)-bearing clay minerals. *Environ. Sci. Technol.* **2017**, *51*, 9817–9825. [[CrossRef](#)]
75. O’Loughlin, E.J.; Traina, S.J.; Sims, G.K. Effects of sorption on the biodegradation of 2-methylpyridine in aqueous suspensions of reference clay minerals. *Environ. Toxicol. Chem.* **2000**, *19*, 2168–2174. [[CrossRef](#)]
76. Ilgen, A.G.; Foster, A.L.; Trainor, T.P. Role of structural Fe in nontronite NAu-1 and dissolved Fe(II) in redox transformations of arsenic and antimony. *Geochim. Cosmochim. Acta* **2012**, *94*, 128–145. [[CrossRef](#)]
77. Segre, C.U.; Leyarowska, N.E.; Chapman, L.D.; Lavender, W.M.; Plag, P.W.; King, A.S.; Kropf, A.J.; Bunker, B.A.; Kemner, K.M.; Dutta, P.; et al. The MRCAT insertion device beamline at the Advanced Photon Source. In *Synchrotron Radiation Instrumentation: Eleventh U.S. National Conference*; Pianetta, P.A., Arthur, J.R., Brennan, S., Eds.; American Institute of Physics: New York, NY, USA, 2000; Volume 521, pp. 419–422.
78. O’Loughlin, E.J.; Kelly, S.D.; Csencsits, R.; Cook, R.E.; Kemner, K.M. Reduction of uranium(VI) by mixed iron(II)/iron(III) hydroxide (green rust): Formation of UO_2 nanoparticles. *Environ. Sci. Technol.* **2003**, *37*, 721–727. [[CrossRef](#)] [[PubMed](#)]
79. Newville, M.; Livinš, P.; Yacoby, Y.; Rehr, J.J.; Stern, E.A. Near-edge x-ray absorption fine structure of Pb: A comparison of theory and experiment. *Phys. Rev. B* **1993**, *47*, 14126–14131. [[CrossRef](#)]
80. Naughton, M.G.M.; James, R.O. Adsorption of aqueous mercury (II) complexes at the oxide/water interface. *J. Colloid Interface Sci.* **1974**, *47*, 431–440. [[CrossRef](#)]

81. Korinek, G.J.; Halpern, J. Effects of complexing on the homogeneous reduction of mercuric salts in aqueous solution by molecular hydrogen. *Can. J. Chem.* **1956**, *34*, 1372–1381. [[CrossRef](#)]
82. Allard, B.; Arsenie, I. Abiotic reduction of mercury by humic substances in aquatic system—an important process for the mercury cycle. *Water Air Soil Pollut.* **1991**, *56*, 457–464. [[CrossRef](#)]
83. Lee, S.; Roh, Y.; Kim, K.W. Influence of chloride ions on the reduction of mercury species in the presence of dissolved organic matter. *Environ. Geochem. Health* **2019**, *41*, 71–79. [[CrossRef](#)]
84. Morse, J.W.; Luther, G.W., III. Chemical influences on trace metal-sulfide interactions in anoxic sediments. *Geochim. Cosmochim. Acta* **1999**, *63*, 3373–3378. [[CrossRef](#)]
85. Frenet-Robin, M.; Ottmann, F. Comparative study of the fixation of inorganic mercury on the principal clay minerals and the sediments of the Loire Estuary. *Estuar. Coast. Mar. Sci.* **1978**, *7*, 425–436. [[CrossRef](#)]
86. Yin, Y.; Allen, H.E.; Li, Y.; Huang, C.P.; Sanders, P.F. Adsorption of mercury(II) by soil: Effects of pH, chloride, and organic matter. *J. Environ. Qual.* **1996**, *25*, 837–844. [[CrossRef](#)]
87. Kim, C.S.; Rytuba, J.J.; Brown, G.E., Jr. EXAFS study of mercury(II) sorption to Fe- and Al-(hydr)oxides II. Effect of chloride and sulfate. *J. Colloid Interface Sci.* **2004**, *270*, 9–20. [[CrossRef](#)] [[PubMed](#)]
88. Amyot, M.; Gill, G.A.; Morel, F.M.M. Production and Loss of Dissolved Gaseous Mercury in Coastal Seawater. *Environ. Sci. Technol.* **1997**, *31*, 3606–3611. [[CrossRef](#)]
89. Amyot, M.; McQueen, D.J.; Mierle, G.; Lean, D.R. Sunlight-induced formation of dissolved gaseous mercury in lake waters. *Environ. Sci. Technol.* **1994**, *28*, 2366–2371. [[CrossRef](#)] [[PubMed](#)]
90. Zhang, H.; Lindberg, S.E. Processes influencing the emission of mercury from soils: A conceptual model. *J. Geophys. Res. Atmos.* **1999**, *104*, 21889–21896. [[CrossRef](#)]
91. Barkay, T.; Miller, S.M.; Summers, A.O. Bacterial mercury resistance from atoms to ecosystems. *FEMS Microbiol. Rev.* **2003**, *27*, 355–384. [[CrossRef](#)]
92. Hobman, J.L.; Wilson, J.R.; Brown, N.L. Microbial mercury reduction. In *Environmental Microbe-Mineral Interactions*; Lovley, D.R., Ed.; ASM Press: Washington, DC, USA, 2000; pp. 177–197. [[CrossRef](#)]
93. Wiatrowski, H.A.; Ward, P.M.; Barkay, T. Novel reduction of mercury(II) by mercury-sensitive dissimilatory metal reducing bacteria. *Environ. Sci. Technol.* **2006**, *40*, 6690–6696. [[CrossRef](#)]
94. Hu, H.; Lin, H.; Zheng, W.; Rao, B.; Feng, X.; Liang, L.; Elias, D.A.; Gu, B. Mercury reduction and cell-surface adsorption by *Geobacter sulfurreducens* PCA. *Environ. Sci. Technol.* **2013**, *47*, 10922–10930. [[CrossRef](#)]
95. Alberts, J.J.; Schindler, J.E.; Miller, R.W.; Nutter, D.E. Elemental mercury evolution mediated by humic acid. *Science* **1974**, *184*, 895. [[CrossRef](#)]
96. Skogerboe, R.K.; Wilson, S.A. Reduction of ionic species by fulvic acid. *Anal. Chem.* **1981**, *53*, 228–232. [[CrossRef](#)]
97. Rocha, J.C.; Junior, É.S.; Zara, L.F.; Rosa, A.H.; dos Santos, A.; Burba, P. Reduction of mercury(II) by tropical river humic substances (Rio Negro)—a possible process of the mercury cycle in Brazil. *Talanta* **2000**, *53*, 551–559. [[CrossRef](#)]
98. Gu, B.; Bain, Y.; Miller, C.L.; Dong, W.; Jiang, X.; Liang, L. Mercury reduction and complexation by natural organic matter in anoxic environments. *Proc. Natl. Acad. Sci. USA* **2011**, *108*, 1479–1483. [[CrossRef](#)] [[PubMed](#)]
99. Chakraborty, P.; Vudamala, K.; Coulibaly, M.; Ramteke, D.; Chennuri, K.; Lean, D. Reduction of mercury (II) by humic substances—Influence of pH, salinity of aquatic system. *Environ. Sci. Pollut. Res. Int.* **2015**, *22*, 10529–10538. [[CrossRef](#)] [[PubMed](#)]
100. Peretyazhko, T.; Charlet, L.; Grimaldi, M. Production of gaseous mercury in tropical hydromorphic soils in the presence of ferrous iron: A laboratory study. *Eur. J. Soil Sci.* **2006**, *57*, 190–199. [[CrossRef](#)]
101. Debure, M.; Grangeon, S.; Robinet, J.C.; Made, B.; Fernandez, A.M.; Lerouge, C. Influence of soil redox state on mercury sorption and reduction capacity. *Sci. Total Environ.* **2020**, *707*, 136069. [[CrossRef](#)] [[PubMed](#)]
102. Poulin, B.A.; Aiken, G.R.; Nagy, K.L.; Manceau, A.; Krabbenhoft, D.P.; Ryan, J.N. Mercury transformation and release differs with depth and time in a contaminated riparian soil during simulated flooding. *Geochim. Cosmochim. Acta* **2016**, *176*, 118–138. [[CrossRef](#)]
103. Ribeiro, F.R.; Fabris, J.D.; Kostka, J.E.; Komadel, P.; Stucki, J.W. Comparisons of structural iron reduction in smectites by bacteria and dithionite: II. A variable-temperature Mössbauer spectroscopic study of Garfield nontronite. *Pure Appl. Chem.* **2009**, *81*, 1499–1509. [[CrossRef](#)]

104. Neumann, A.; Sander, M.; Hofstetter, T.B. Redox properties of structural Fe in smectite clay minerals. In *Aquatic Redox Processes*; Tratnyek, P.G., Grundl, T.J., Haderlein, S.B., Eds.; American Chemical Society: Washington, DC, USA, 2011; Volume 1071, pp. 361–379.
105. Stucki, J.W. A review of the effects of iron redox cycles on smectite properties. *Comptes. Rendus. Geosci.* **2011**, *343*, 199–209. [[CrossRef](#)]
106. Jones, A.M.; Murphy, C.A.; Waite, T.D.; Collins, R.N. Fe(II) interactions with smectites: Temporal changes in redox reactivity and the formation of green rust. *Environ. Sci. Technol.* **2017**, *51*, 12573–12582. [[CrossRef](#)]
107. Entwistle, J.; Latta, D.E.; Scherer, M.M.; Neumann, A. Abiotic degradation of chlorinated solvents by clay minerals and Fe(II): Evidence for reactive mineral intermediates. *Environ. Sci. Technol.* **2019**, *53*, 14308–14318. [[CrossRef](#)]

Publisher's Note: MDPI stays neutral with regard to jurisdictional claims in published maps and institutional affiliations.



© 2020 by the authors. Licensee MDPI, Basel, Switzerland. This article is an open access article distributed under the terms and conditions of the Creative Commons Attribution (CC BY) license (<http://creativecommons.org/licenses/by/4.0/>).